# Big Bang nucleosynthesis considering additional light neutrino families

**by Raphael Roth**

11.10.2007

## Contents

**Abstract**

In this report, Big Bang nucleosynthesis calculations are used to test the impact of additional neutrino flavors on primordial abundances of light elements. Especially primordial $^4$He is a sensitive probe for counting the neutrino number, since nearly all free neutrons were bound to this nucleus while the universe cooled down.

# 1 Introduction

At the time when Einstein developed his theory on General Relativity, the framework for modern cosmology was born. Friedmann's solution to the field equation, the Friedmann equations (see section 2.1), describe an adiabatically expanding universe. Starting from an extremely hot quark-gluon plasma, temperature decreases quickly due to fast space expansion. After about 3 seconds, when only protons and neutrons existed, one of the most important process occurred: the synthesis of nuclei. The results of these process, the primordial element abundances, strongly affected further cosmic evolution and can still be observed in old stars and gas clouds.

Big Bang nucleosynthesis (BBN, or SBBN for standard BBN) is one of the most sensitive probes available for physics going beyond the standard model. In this case, "standard model" means specifically that we consider exactly 3 neutrino families ($N_\nu = 3$). The concordance between numerical predictions and observational data of light element abundances like $^1$H, $^2$H, $^3$H, $^3$He, $^4$He and $^7$Li reflects the overall success of the standard big bang cosmology. Due to the robustness of BBN, changes from the standard model are likely to upset this agreement and are therefore tightly constrained.

The $^4$He abundance, in particular, is commonly used as a sensitive probe of new physics (see e.g. [5] - [9]). This is because nearly all free neutrons end up in $^4$He during BBN. The neutron number, respectively the neutron-to-proton ratio, is very sensitive to the temperature at the so-called weak freeze-out, which in turn depends on the number of neutrino families $N_\nu$. This is due to the competition between weak reaction rates and Hubble expansion, see section 2.2.

On the other hand, BBN also depends on the baryon number density $\eta = n_b/n_\gamma$. Therefore, a meaningful limit on $N_\nu$ requires both a lower bound to $\eta$ (WMAP data are commonly used) and an upper bound to the primordial $^4$He mass fraction. The method for neutrino number counting will be discussed more precisely in section 4. For all these numerical calculations, a full nuclear network code was used, which has been modified for this purpose.

# 2 Physics of the expansion

## 2.1 Evolution of space-time in GR

Standard Big Bang cosmology assumes spatial isotropy and homogeneity, the so-called 'Cosmological Principle' (Milne 1935). This is not only a theoretical construct, since observations in the last few decades provided empirical justifications for this assumption. Despite small temperature/density - inhomogeneities found in the cosmic microwave background (CMB), and the filament structure in galaxy distribution, the universe conforms to this postulate when the relevant scales are considered (observational universe = several thousand Mpc).

For an isotropic and homogeneous evolving space-time with co-moving spherical coordinates, the distance between two points is given by the Robertson-Walker metric

$$ds^2 = g_{\mu\nu}dx^\mu dx^\nu = dt^2 - R^2(t)\left[\frac{dr^2}{1-kr^2} + r^2\left(d\Theta^2 + \sin^2\Theta d\Phi^2\right)\right] \quad , \quad (1)$$

where $R(t)$ denotes the cosmic scale factor and $k$ the algebraic sign of the curvature. By making use of Einstein's field equation, connecting space-time geometry ($g_{\mu\nu}$ and $R_{\mu\nu}$) with the energy-momentum tensor $T_{\mu\nu}$ ,

$$R_{\mu\nu} - \frac{1}{2}g_{\mu\nu}R + \Lambda g_{\mu\nu} = -\frac{8\pi G}{c^4}T_{\mu\nu} \quad , \quad (2)$$

Friedmann succeeded in deriving 3 equations of motion for $R(t)$; The famous Friedmann-Lemaitre equations are:

$$\ddot{R} = -\frac{4\pi}{3c^2}(\rho_\epsilon + 3P)GR + \frac{1}{3c^2}\Lambda R \quad , \quad (3)$$

$$\frac{\dot{R}}{R}^2 = H(t)^2 = \frac{8\pi G}{3c^2}\rho_\epsilon - \frac{kc^2}{R^2} + \frac{1}{3c^2}\Lambda \quad , \quad (4)$$

$$\frac{d(\rho_\epsilon R^3)}{dt} + P\frac{dR^3}{dt} = 0 \quad . \quad (5)$$

Here, $\rho_\epsilon$ denotes the total relativistic energy density $\rho_\epsilon = u + \rho c^2$ and $\rho$ the mass density. For the case of a not vanishing $\dot{R}$, only 2 of these equations are independent. The cosmological constant $\Lambda$, acting like an integration constant in Eq. (2), can also be interpreted as an energy density $\rho_\Lambda = \frac{\Lambda}{8\pi G}$. This cosmological constant, nowadays assumed to be small but non-zero, disconnects geometry and dynamics of the so-called world-models, resulting from Eq. (3) - (5). Depending on the choice of parameters, many world

models are possible. Eq. (4) can be interpreted in the non-relativistic limit as an energy conversation law, Eq. (5) as the first law of thermodynamics, $dQ = dU + PdV = 0$, in an adiabatic expansion of an ultra-relativistic gas (chemical potential $\mu = 0$ for all particles).

In the non-relativistic limit $E/m \ll 1$ (matter dominated epoch), Eq. (5) leads to $\rho \propto R^{-3}$, reflecting the dilution of density due to the expanding volume of a sphere. In the relativistic case ($mc^2 \ll kT$), applicable to the early universe, the pressure reads $P = \frac{\rho_\epsilon}{3}$ and we get an additional $R^{-1}$ because of the redshift of momentum by expansion. This leads to

$$\rho_\epsilon R^4 = const \quad . \tag{6}$$

Considering zero curvature, this means $\dot{R} = R^{-1}$ and therefore

$$R(t) = \alpha t^{\frac{1}{2}} \quad . \tag{7}$$

Immediately after the big bang, when $kT \gtrsim 200$ MeV, quarks and gluons are believed to be asymptotically free in a very dense plasma. With the ongoing expansion, quarks soon combine to baryons. Since particle-antiparticle pairs can be created by collision of 2 photons, all particles exist with $mc^2 \ll kT$. With temperatures $\sim 1$ MeV, photons, nucleons, electrons, positrons and neutrinos (+antiparticles) are in thermal equilibrium due to reactions like $\gamma + \gamma \rightleftharpoons e^+ + e^-$, $\nu_e + \nu_e \rightleftharpoons e^+ + e^-$, $e^- + p \rightleftharpoons n + \nu_e$ and $e^+ + n \rightleftharpoons p + \bar{\nu_e}$, leading to a chemical equilibrium between the participants. This is the point where our calculations set in.

## 2.2 Derivation of the relevant astrophysical parameters

Here follows a derivation of the necessary relations describing the evolution of temperature, density etc. during the expansion shortly after big bang. For more details see [1], [2] and [4].

For an ultra-relativistic gas, pressure behaves like

$$P = \frac{1}{3}\rho_\epsilon = \frac{1}{3}u = \frac{1}{3}\frac{g}{2}aT^4 \quad . \tag{8}$$

The total statistical weight $g$ can be expressed as a sum of the $g_i$ from the participating particles ($g_\gamma = g_{e^+} = g_{e^-} = 2$ and $g_\nu = g_{\bar{\nu}} = 1$).

$$g = \sum_{bosons} g_i + \frac{7}{8} \sum_{fermions} g_i = 2 + \frac{7}{8} \cdot (2+2+1+1+1+1+1+1) = \frac{43}{4} \tag{9}$$

At this point, the expression for the standard case ($N_\nu = 3$) will be expanded to hypothetical additional (light) neutrino families $\Delta N_\nu$. So $N_\nu = 3 + \Delta N_\nu$. In contrast to the standard derivation that can be found in common literature, this variable $\Delta N_\nu$ will be carried on until we find the final relations. This will then be our "tool" for studying the influence of neutrino number on BBN. Applying this notation leads to

$$g = \frac{43}{4} + \frac{7}{8}\Delta N_\nu \cdot (1+1) = \frac{43}{4} + \frac{7}{4}\Delta N_\nu \quad . \tag{10}$$

The nucleons do not appear in this expression because $m_{nucleons}c^2 \gg kT$, so they obey Maxwell-Boltzmann statistics and therefore $P = nkT$. Since this term is linear in $T$, it is negligible for high temperatures. The electron/positron ($\bar{\mu_{e^+}} = \bar{\mu_{e^-}} = 0$) reactions with nucleons lead to $\bar{\mu_n} = \bar{\mu_p}$. This can be used to express the neutron to proton ratio

$$\frac{n_n}{n_p} \equiv \frac{n}{p} = exp\left(\frac{\Delta m c^2}{kT}\right) \quad , \tag{11}$$

where $\Delta m$ denotes the neutron-proton mass difference.

Once temperature drops below $\sim$ 1 MeV , electrons are not energetic enough to overcome the mass difference between neutrons and protons via $e^-$-capture. Also the $e^+ + e^-$ pair creation ceases and thus positron capture on neutrons, since the photon energy falls below the threshold. At the time when these processes disappear, neutrinos cannot thermally interact anymore with the other particles. This phase is called *weak freeze-out* (or *weak decoupling*), from this time on, neutrinos and photons have different temperatures. The proton to neutron ratio is frozen out at $\frac{n}{p} = exp\left(-\frac{\Delta m c^2}{kT_{frz}}\right)$. From this time on the ratio can only be changed via beta-decay of the neutrons.

For ultra-relativistic particles, the entropies are given by $S_{boson} = \frac{g_b}{2}\frac{4}{3}aT^3V$ and $S_{fermion} = \frac{7}{8}\frac{g_f}{2}\frac{4}{3}aT^3V$. To calculate $T_\nu/T_\gamma$, we have to consider the entropy at $T_{frz}$, which is equal before and after the freeze-out:

$$\left(\frac{43}{8} + \frac{7}{8}\Delta N_\nu\right) aT_\nu^3 V = aT_\gamma^3 V + \frac{7}{8}\left(\frac{6 + 2\Delta N_\nu}{2}\right) aT_\nu^3 V$$

$$\Rightarrow \frac{T_\gamma}{T_\nu} = \left[\left(\frac{43}{8} + \frac{7}{8}\Delta N_\nu\right) - \frac{7}{8}\left(\frac{6 + 2\Delta N_\nu}{2}\right)\right]^{\frac{1}{3}} = \left(\frac{11}{4}\right)^{\frac{1}{3}} \quad . \tag{12}$$

This ratio is independent of the number of neutrino families. We see that the photon temperature is higher than the neutrino temperature, that is because the annihilatinon of the electron/positron pairs heated up the photon bath.

Since $u_{i,bosons} = \frac{g_i}{2} u_\gamma$ and $u_{i,fermions} = \frac{7}{8}\frac{g_i}{2} u_\gamma$, we can write

$$\begin{aligned} u_{tot} &= aT_\gamma^4 + \frac{7}{8}\left(\frac{6+2\Delta N_\nu}{2}\right) aT_\nu^4 \\ &= \left(1 + \left(\frac{21+7\Delta N_\nu}{8}\right)\left(\frac{T_\nu}{T_\gamma}\right)^4\right) aT_\gamma^4 \quad . \end{aligned} \tag{13}$$

Plugging (12) in (13), we finally get

$$u_{tot} = \underbrace{\left[1 + \left(\frac{21+7\Delta N_\nu}{8}\right)\left(\frac{11}{4}\right)^{-\frac{4}{3}}\right]}_{\frac{g}{2}} aT_\gamma^4 \tag{14}$$

and therefore, the new value for $g$ after the weak freeze-out is:

$$g = 2\left[1 + \left(\frac{21+7\Delta N_\nu}{8}\right)\left(\frac{11}{4}\right)^{-\frac{4}{3}}\right] \quad . \tag{15}$$

Plugging in the numbers in (15) shows that g drops from 10.75 to 3.3626 ($N_\nu = 3$) respectively from 12.5 to 3.817 ($N_\nu = 4$). The steep drop in g is illustrated in Fig. 1.

Making use of the adiabatic invariant of the photon gas and the expression for the expansion rate, one gets a relation between time and temperature (after the phase transitions) for the photon gas:

$$\begin{aligned} t &= \left(\frac{3c^2}{16\pi G a}\right)^{\frac{1}{2}} g^{-\frac{1}{2}} T^{-2} \\ \Rightarrow T &= \left(\frac{3c^2}{16\pi G a}\right)^{\frac{1}{4}} g^{-\frac{1}{4}} t^{-\frac{1}{2}} \quad , \end{aligned} \tag{16}$$

with $a = \frac{4\sigma}{c} = 7.5657 \times 10^{-16}$, $G = 6.67259 \times 10^{-11}$. Plugging in $g$ from (15) leads to the important relation:

$$T = \left(\frac{3c^2}{16\pi G a}\right)^{\frac{1}{4}} \left(2\left[1 + \left(\frac{21+7\Delta N_\nu}{8}\right)\left(\frac{11}{4}\right)^{-\frac{4}{3}}\right]\right)^{-\frac{1}{4}} t^{-\frac{1}{2}} \quad . \tag{17}$$

This relation will be needed as input parameter for the nucleosynthesis network code.

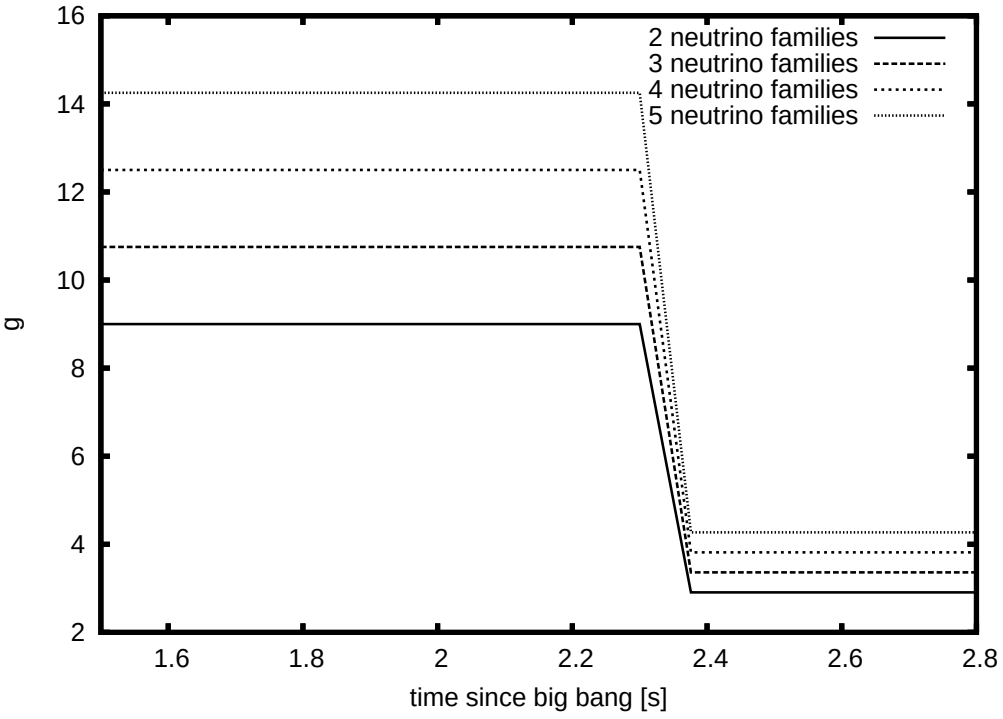


Figure 1: Evolution of $g$ during freeze-out

The next step is to calculate the weak freeze-out temperature. We can guess that it will be between $T = 1.29$ MeV (mass difference between neutron and protons) and $T = 0.511$ MeV (mass of electron). Finding this temperature $T_{frz}$ would require a self-consistent numerical calculation, using a network code which can handle weak reactions. Since our code is not able to do this, an analytical approximation is used (see e.g. [4]). The freeze-out of a reaction means that the expansion rate $H(T)$ becomes larger than the scattering rate $\Lambda_{scatt}(T)$. So, at $T = T_{frz}$, we have the condition

$$H(T_{frz}) \backsimeq \Lambda_{scatt}(T_{frz}) \quad , \tag{18}$$

$$H = \sqrt{\frac{8\pi\rho\,(T)}{3M_p^2}} \simeq 1.66 g^{\frac{1}{2}} T^2 M_p^{-1} \quad ,$$

$$\Lambda_{scatt} = \frac{7}{60}\pi \left(1 + 3g_A^2\right) G_F^2 T^5 \quad ,$$

where $g_A \approx 1.26$, $G_F = 1.166 \times 10^{-5}$ GeV $^{-2}$ and $M_p = 1.2209 \times 10^{19}$ GeV c$^{-2}$. Using condition (18) leads to

$$T_{frz} = \left[ \frac{\sqrt{\frac{8}{90}\pi^3} g^{\frac{1}{2}}}{\frac{7}{60}\pi \left(1 + 3g_A^2\right) G_F^2 M_p} \right]^{1/3} \approx \left( \frac{0.785}{G_F^2 M_p} \right)^{1/3} g^{\frac{1}{6}} \quad . \tag{19}$$

Unfortunately, (19) leads to a value that is too high ($\sim$ 1.157 MeV for $N_\nu = 3$) compared to literature values (commonly around 0.8 MeV [2]). But since we know $T_{frz} \propto g^{\frac{1}{6}}$ (g from (10)), we can determine $T_{frz}$ requiring that the assumption $n/p = 1/6$ ($N_\nu = 3$) is fulfilled:

$$exp\left( \frac{-1.293 \text{ MeV}}{T_{frz}} \right) = \frac{1}{6}$$

$$\Rightarrow T_{frz} = 0.7216 \text{ MeV} \quad . \tag{20}$$

Using the proportionality $T_{frz} \propto g^{\frac{1}{6}}$, we can write

$$T_{frz}^{(3+\Delta N_\nu)} = T_{frz}^{(3)} \left( \frac{g^{(N_\nu = 3+\Delta N_\nu)}}{g^{(N_\nu = 3)}} \right)^{\frac{1}{6}} = T_{frz}^{(3)} \left( 1 + \frac{7}{43} \Delta N_\nu \right)^{\frac{1}{6}} \tag{21}$$

This means that the weak freeze-out occurs at a higher temperature, the more additional neutrino families we have (e.g. $T_{frz} = 0.7400$ MeV for $N_\nu = 4$). Plugging in (21) in (11), we can calculate the ratio $n/p\,(\Delta N_\nu)$ at the freeze-out:

$$\frac{n}{p} = exp\left( \frac{-1.293 \text{ MeV}}{T_{frz}^{(3)} \left(1 + \frac{7}{43}\Delta N_\nu\right)^{\frac{1}{6}}} \right) \quad . \tag{22}$$

For example, this ratio (= 0.1666 for $N_\nu = 3$ as we assumed) increases to $\approx 0.174$ for $N_\nu = 4$.

The last parameter to be determined is the time when the freeze-out occurs. This can be done using (17) and (21):

$$t_{start} = \left[ \frac{\frac{T_{frz} \cdot 10^6}{k}}{\left(\frac{3c^2}{16\pi G a}\right)^{\frac{1}{4}} g^{-\frac{1}{4}}} \right]^{-2} \quad . \tag{23}$$

Together with (17), (23) describes a behavior as illustrated in Fig. 2.

The higher pressure of the plasma resulting from additional neutrino families is leading to an accelerated expansion. In literature, one defines a dimensionless cosmic "speed-up" factor $\xi = H_{new}/H_{std}$, where H denotes the

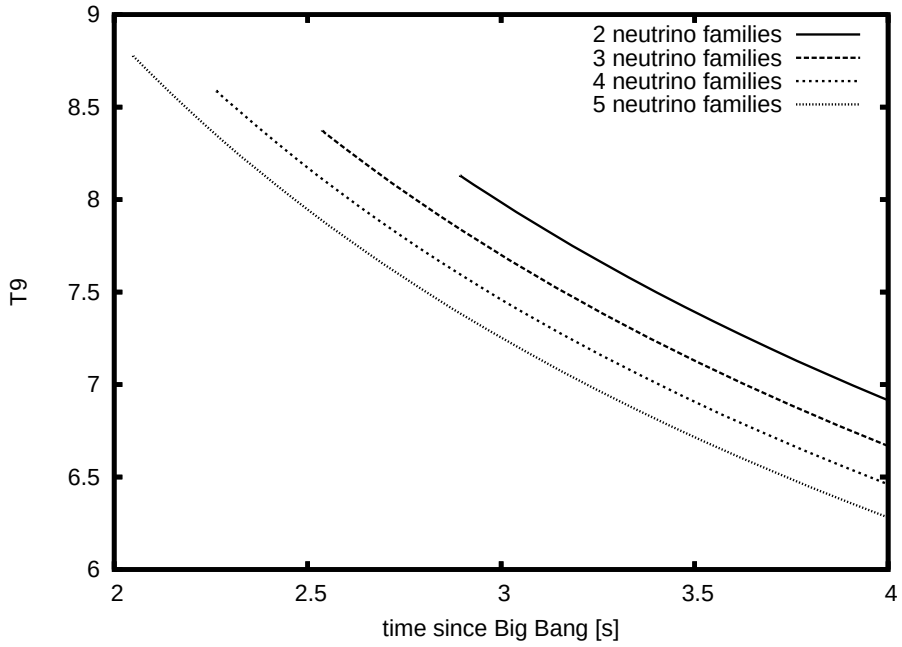


Figure 2: Temperature behavior near weak freeze-out for different neutrino numbers, starting at $T_{frz}$.

Hubble parameter $\dot{R}/R$. The expansion rate itself is given by the solutions of the Friedmann equations and is $\propto \sqrt{\rho} \propto g$. So the speed-up factor is therefore:

$$\xi = \sqrt{1 + 7\Delta N_\nu/43} \quad . \tag{24}$$

The strength of the (S)BBN is the fact that it mainly depends (besides $N_\nu$) only on one free parameter, the baryon-to-photon ratio $\eta = \frac{n_b}{n_\gamma}$, with $n_\gamma = 2.404\frac{k^3T^3}{\pi^2\hbar^3c^3}$. Therefore, the baryon density $\rho_b$ and the number density $n_{bar}$ are

$$\begin{aligned} n_{bar} &= \eta \cdot n_\gamma = 2.404 \cdot \eta \frac{k^3T^3}{\pi^2\hbar^3c^3} \quad , \\ \rho_b &= n_b m_u = 3.376 \times 10^4 \eta T_9^3 g cm^{-3} \quad . \end{aligned} \tag{25}$$

This is true if we neglect the small mass difference between proton and neutron compared to the atomic mass unit. The parameter $\eta_{10} \equiv \eta \times 10^{10}$ has long been assumed to be around $\sim 4$, but since data from WMAP has been analyzed [11], it is more likely that $\eta_{10} \approx 6$ (see section 5).

To summarize: We have a set of input parameters for our network code to calculate primordial abundances. They are:

- $\eta$ (from WMAP) ,
- $N_\nu$ ,
- $T_9(t)$ from (17) ,
- $\rho_b(t)$ from (25) ,
- initial $n/p$ ($t = t_{start}$) from (22) .

Table 1 shows the most important numerical values of some parameters, computed for the cases $N_\nu = 2, 3, 4$ and 5

Table 1: Some numerical values of the equations discussed in section 2.2

| $N_\nu$ | $g_{before}$ | $g_{after}$ | $T_{frz}[MeV]$ | $t_{start}[s]$ | $n/p$ ($t_{start}$) |
|---|---|---|---|---|---|
| 2 | 9.00 | 2.908 | 0.701 | 2.894 | 0.158 |
| 3 | 10.75 | 3.363 | 0.722 | 2.536 | 0.167 |
| 4 | 12.50 | 3.817 | 0.740 | 2.264 | 0.174 |
| 5 | 14.25 | 4.271 | 0.756 | 2.049 | 0.181 |

# 3 Big Bang nucleosynthesis beyond the standard model

## 3.1 Numerical treatment

In general, nucleosynthesis calculations are divided into two categories, (a) nucleosynthesis during the hydrostatic burning stages of stellar evolution and (b) nucleosynthesis in explosive events. The difference is obvious: in (a), temperature and pressure are given by an equilibrium condition, while in (b), those 2 parameters result from hydrodynamics (i.e. supernovae, Hubble-expansion...). Of course, our system belongs to the category (b), since the solutions of the Friedmann equations (3) - (5) determines temperature and pressure of this non-equilibrium scenario (see Eq. (17) and (25)) . Let us now examine how nuclear reaction rates are calculated, although strongly simplified here (see [10] for more details).

Consider two types of particles $i$ and $j$, with number densities $n_i$ and $n_j$. The cross section for the reaction $i(j,o)m$ at a given relative velocity $v$ is defined by

$$\sigma = \frac{number\ of\ reactions\ target^{-1}\ sec^{-1}}{flux\ of\ incoming\ projectiles} = \frac{r/n_i}{n_j v} \quad . \tag{26}$$

The number of reactions per $sec$, $r$, and $cm^{-3}$ is then given by

$$r_{i;j} = \int \sigma \cdot |\overrightarrow{v_i} - \overrightarrow{v_j}| \, dn_i dn_j \quad , \tag{27}$$

where $dn_i$ and $dn_j$ denote the statistical distribution of the particles. For nuclei in our astrophysical plasma, we use the Maxwell-Boltzmann distribution

$$\begin{aligned} dn_j &= n_j (\frac{m_j}{2\pi kT})^{3/2} exp(-\frac{m_j v_j^2}{2kT}) d^3 v_j \\ &= n_j \Phi(\overrightarrow{v_j}) d^3 v_j \quad . \end{aligned}$$

We then find

$$\begin{aligned} r_{i;j} &= n_i n_j \int \sigma(|\overrightarrow{v_i} - \overrightarrow{v_j}|) \, |\overrightarrow{v_i} - \overrightarrow{v_j}| \, \Phi(\overrightarrow{v_i}) \Phi(\overrightarrow{v_j}) d^3 v_i d^3 v_j \quad , \\ r_{i;j} &=: n_i n_j \int \langle \sigma v \rangle_{i;j} \quad . \end{aligned} \tag{28}$$

Doing some variable transformations allows us to express $\langle \sigma v \rangle_{i;j}$ with an energy integral, which only depends on the temperature $T$

$$\langle \sigma v \rangle (T) = \left( \frac{8}{\mu \pi} \right)^{1/2} \frac{1}{kT^{3/2}} \int_0^\infty E \sigma(E) \exp(-E/kT) dE \quad . \tag{29}$$

To obtain the nuclear reaction rate, we have to know the cross section $\sigma(E)$, either from experiments, theoretical models or relations like e.g. detailed balance for reverse reactions etc..

The next step is to consider other reactions than fusion, like photodisintegration, lepton captures, and $\beta^{\pm}$-decays. For photodisintegration, we again start with (27), but then use the Planck distribution for $dn_\gamma$.

$$r_{i\gamma} = n_i \lambda_{i;\gamma,o}(T) \tag{30}$$

Here, the "decay"-constant $\lambda$ only depends on temperature, since $n_\gamma \propto T^3$. Analogous, we get an expression for electron/positron-capture

$$r_{i;e} = n_i \lambda_{i;e}(\rho Y_e, T) \quad . \tag{31}$$

Notice that $\lambda$ depends on temperature and the electron abundance $Y_e$ (in this report, $Y_i$ always denote abundance while $X_i$ denote mass fraction). Finally, we obtain a similar expression for normal decays like alpha/beta - decays. Using $\lambda_i = ln(2)/\tau_{1/2}$, the reaction rate simply reads

$$r_i = \lambda_i n_i \quad . \tag{32}$$

Neutrino reactions would be treated similarly, but they are not implemented in the used code. To actually calculate the abundances of the nuclei, we use $(\frac{\delta n_i}{\delta t})_\rho = r_{i;j}$ and plug in the definition of relative abundance $Y_i = \frac{n_i}{\rho N_A}$. Like that, we can merge all the reactions discussed above into one set of differential equations for each nucleus $i$

$$\dot{Y}_i = \sum_j N_j^i \lambda_j Y_j + \sum_{i,k} \frac{N_{j,k}^i}{1+\delta_{jk}} \rho N_A \langle \sigma v \rangle_{j;k} Y_j Y_k \quad . \tag{33}$$

The term $\delta_{jk}$ is to avoid double counting reactions between 2 identical nuclei. $N^i$ is the number of particles created/destroyed in a reaction. Eq. (33) is numerically solved by a finit difference method

$$\frac{\vec{Y}(t+\Delta t) - \vec{Y}(t)}{\Delta t} = (1-\Theta)\dot{\vec{Y}}(t+\Delta t) + \Theta \dot{\vec{Y}}(t) \quad . \tag{34}$$

Using for instance $\Theta = 0$, (34) represents the implicit backward Euler method, which then makes (34) identical to

$$\vec{Z}(t+\Delta t) \equiv \frac{\vec{Y}(t+\Delta t) - \vec{Y}(t)}{\Delta t} - \dot{\vec{Y}}(t+\Delta t) \quad . \tag{35}$$

This can be solved using the Newton-Raphson method. The change in abundance is then

$$\Delta \vec{Y} = \left( \frac{\delta \vec{Z}(t+\Delta t)}{\delta \vec{Y}(t+\Delta t)} \right)^{-1} \vec{Z} \quad . \tag{36}$$

Where $\frac{\delta \vec{Z}}{\delta \vec{Y}}$ is the Jacobian of $\vec{Z}$. Iteration continues until $\vec{Y}(t+\Delta t)$ converges.

In our code the timestep is dynamically coupled to the evolution of the abundances. At the beginning, $\Delta t$ is $\approx 10^{-9}$ s, increasing as the $\dot{Y}_i$'s decrease with time until abundances freeze out.

## 3.2 Basic BBN reactions

In this chapter, we discuss basic reactions that occur during BBN. For better understanding of this mechanisms, several calculations have been made using our code and input parameters (see Fig. (3)-(7)). Our results for the standard Big Bang are in general agreement with literature values.

As mentioned above, after the weak freeze-out, the n/p ratio decreases only because of the beta-decay of the neutron. Since photons are energetic enough, they destroy immediately all the $^2$H that has been built by neutron capture on protons. Only after $\sim$ 150 s when $T_9 := T/10^9$ K$\approx$ 1.1, a substantial abundance of $^2$H exist and nucleosynthesis can proceed. Thus, the

onset of nucleosynthesis is due to the Q-value of $^1$H(n, $\gamma$)$^2$H (Q=2.3 MeV). The more neutrino families we have, the earlier begins the production of $^2$H (because of the lower temperature), see Fig. 3.

Subsequently, further neutron-, proton- and light nuclei ($^2$H) captures form heavier nuclei like $^3$H, $^3$He and $^4$He. That is why the abundance of deuterium reaches its maximum at around $t \approx 250s$ and then drops quickly. The reaction chain contains the sequence of two body reactions:

| | | |
|---|---|---|
| $^1$H(n,$\gamma$)$^2$H | | |
| $^2$H(p, $\gamma$)$^3$He | $^2$H($^2$He,n)$^3$He | $^2$H($^2$H,p)$^3$H |
| $^3$H($^2$H,n)$^4$He | $^3$H($^4$He, $\gamma$)$^7$Li | |
| $^3$He(n,p)$^3$H | $^3$He($^2$H,p)$^4$He | $^3$He($^4$He, $\gamma$)$^7$Be |
| $^7$Li(p,$^4$He)$^4$He | $^7$Be(n,p)$^7$Li | |

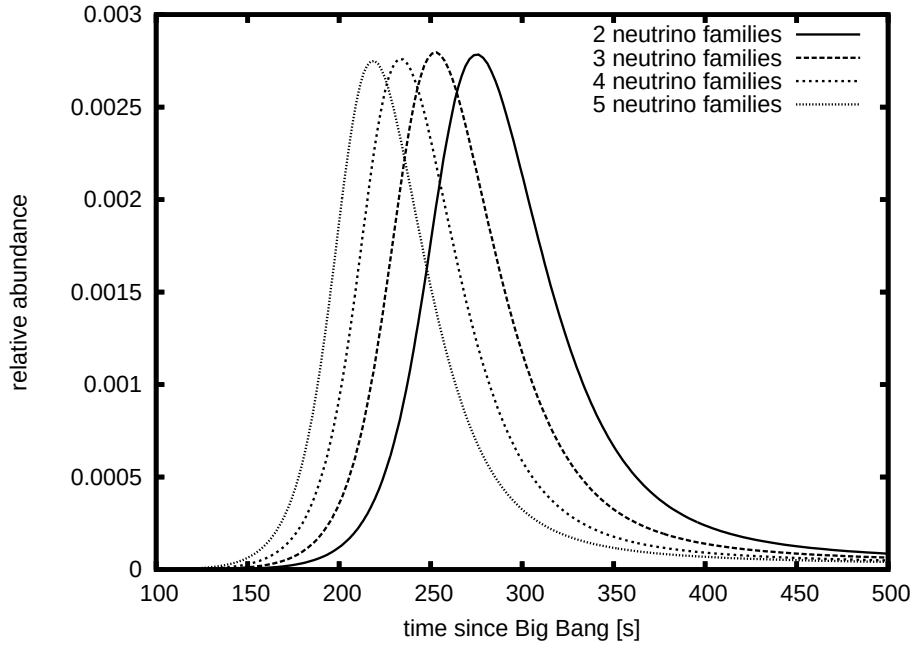


Figure 3: Time evolution of $^2$H abundance

Most of the neutrons are finally bound in $^4$He, because of its large binding energy ($\Delta_{^4\mathrm{He}} = 28.3$ MeV). Since the gap in the bound nuclei at A=5 and A=8 inhibits the formation of nuclei beyond A=4, only traces of $^7$Li and $^7$Be are made. Using this fact, the final $^4$He mass fraction can be approximated assuming all neutrons being bound to this nucleus

$$X_{\alpha,primordial} \approx \frac{2X_n/X_p}{1 + X_n/X_p} \approx 0.25 \quad . \tag{37}$$

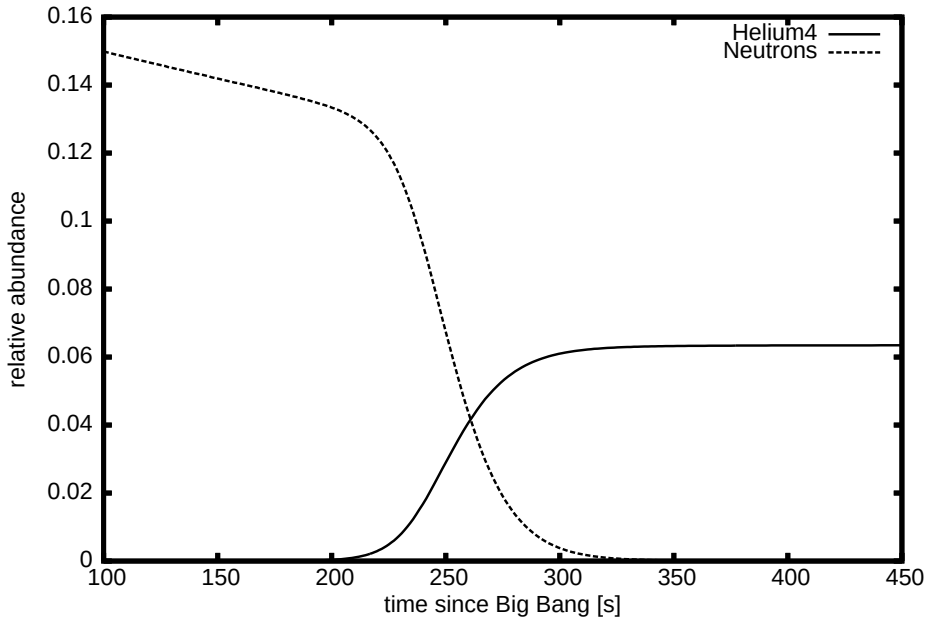


Figure 4: Binding of free neutrons in $^4$He

Since we have many more protons than neutrons ($\approx 1/7$ at the time when nucleosynthesis starts) , many protons remain unbound at the time when all free neutrons have been captured. That is why $^1$H is the most abundant relict of BBN ($Y_H \approx 0.745$). Fig. 5 shows quantitatively the evolution of abundances of the light elements as result of the reaction listed above.

## 3.3 Abundance dependence on $\eta$

As mentioned before, all of these processes depend mainly (in SBBN) on the baryon-to-photon ratio $\eta$. If we have large $\eta$, i.e. a high baryon density, this leads to a higher number of capture reactions on $^2$H and $^3$He. This, consequently, leads to a higher amount of $^4$He but leaving of course less $^2$H and $^3$He. The behavior of $^7$Li is more complex, since it is produced in two different channels. For low baryon densities, $^7$Li is produced via $^3\mathrm{H}(\alpha,\gamma)^7\mathrm{Li}$, but at high densities, it is destroyed by $^7\mathrm{Li}(\mathrm{p},\ \alpha)^4\mathrm{He}$. On the other hand, increasing $\eta$ also leads to overproduction of $^7$Be because of a higher rate of $^3\mathrm{He}(\alpha,\gamma)^7\mathrm{Be}$. This unstable $^7$Be subsequently decays to $^7$Li. The minimum of the $^7$Li abundance is about $10^{-10}$ and lies between $2 < \eta_{10} < 4$. The behavior of the abundances with changing $\eta$ is plotted in Fig. 6 and 7.

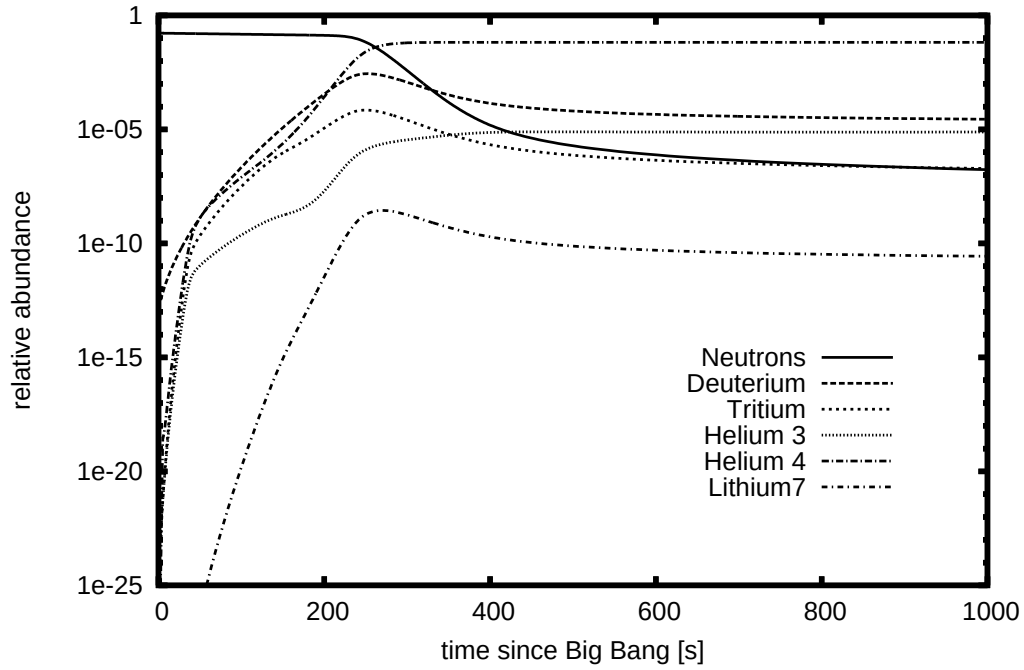


Figure 5: Overview of abundance evolution of all light elements (except protons) in SBBN for a fixed value of $\eta$. Most of the processes occur in the time between 200s and 400s after BB, and after $\sim$ 1000s nearly all abundances reach its final values. Note that the $^7$Li abundance will still grow with time due to the decay of $^7$Be

# 4 Neutrino-counting with BBN

In this section, we have varied $\Delta N_\nu$ to find a upper limit for the number of light neutrino families. As already discussed in section 2.2, additional neutrino families sensitively affect BBN, especially the $^4$He abundance. This is because of (i) earlier weak freeze-out and therefore higher $n/p$ ratio [Eq. (22)] and (ii) lower temperature after freeze-out [Eq. (17)]. The other elements that are produced in BBN are not so sensitive to a variation of $N_\nu$ (see Tab. 2 for final abundances), and additionally, their relics are more difficult to observe nowadays with sufficient accuracy.
To (i): As seen in Eq. (37), the $^4$He mass fraction depends on the $n/p$ ratio at the time when nucleosynthesis starts and not directly on the $n/p$ ratio at freeze-out. One could argue that with an increasing $\Delta N_\nu$ and therefore the earlier freeze-out, the neutrons have more time to decay until nucleosynthesis starts. But $t_{start}$ only differs by $\sim$ 0.2s for each additional neutrino family.

Table 2: Final abundances $Y_i$ of BBN. Note that $^3$H is unstable, so the abundance below denotes the value right after BBN ($t \approx 10^5$ s). The abundance of $^7$Li already contains the decayed $^7$Be. The second table lists the relative changes of $Y_i$ compared to the standard case $N_\nu = 3$.

| *Nuclei* | $N_\nu = 2$ | $N_\nu = 3$ | $N_\nu = 4$ | $N_\nu = 5$ |
|---|---|---|---|---|
| $^1$H | 0.7651 | 0.7460 | 0.7290 | 0.7139 |
| $^2$H | 2.162E-05 | 1.996E-05 | 1.778E-05 | 1.654E-05 |
| $^3$H * | 6.247E-08 | 5.817E-08 | 5.212E-08 | 4.869E-08 |
| $^3$He | 8.990E-06 | 8.684E-06 | 8.221E-06 | 7.938E-06 |
| $^4$He | 5.873E-02 | 6.349E-02 | 6.775E-02 | 7.150E-02 |
| $^7$Li | 2.2225E-10 | 2.336E-10 | 2.351E-10 | 2.407E-10 |
| *Nuclei* | $Y_i^{N_\nu=2}/Y_i^{N_\nu=3}$ | $Y_i^{N_\nu=3}/Y_i^{N_\nu=3}$ | $Y_i^{N_\nu=4}/Y_i^{N_\nu=3}$ | $Y_i^{N_\nu=5}/Y_i^{N_\nu=3}$ |
| $^1$H | 1.026 | 1.000 | 0.977 | 0.957 |
| $^2$H | 1.083 | 1.000 | 0.891 | 0.829 |
| $^3$H * | 1.074 | 1.000 | 0.896 | 0.837 |
| $^3$He | 1.035 | 1.000 | 0.945 | 0.914 |
| $^4$He | 0.925 | 1.000 | 1.067 | 1.126 |
| $^7$Li | 0.951 | 1.000 | 1.006 | 1.030 |

This is, compared to the neutron half life $\tau_{1/2} \approx 614$s, very short and therefore this impact is negligible ($\Delta n/p \approx 10^{-4}$), compared to the effect resulting from Eq. (22). But as can be seen in Fig. 8, the differences in $n/p$ slightly shrink until nucleosynthesis starts. It is also quite clear that a higher $N_\nu$ ($\Rightarrow$ more neutrons) leaves less protons at the end of BBN than a low $N_\nu$ (see Tab. 2).

To (ii): As derived in section 2.2, the factor in front of $t^{-1/2}$ in relation (17) changes due to $g(\Delta N\nu)$. For example, $N_\nu = 4$ leads to a factor 12.922 instead of 13.336 for the standard case. This affects mainly the time when deuterium starts to build up, but has little effect on the final $X_\alpha$. As Fig. 9 shows, a low $N_\nu$ allows earlier $^4$He production, but then ceases at around 260 sec when all "fuel" has been exhausted. But with a higher $N_\nu$, nucleosynthesis continues for additional $\sim$ 20s (since there are still free neutrons available), therefore $X_\alpha$ exceeds the value at low $N_\nu$ (Fig. 10). Considering all these effects, one can parameterize $X_\alpha$ with suitable numbers A,B,C and D::

$$X_\alpha = A + B(N_\nu - 3) + Cln(\eta_{10}) + D(\tau_n - 887) \quad . \tag{38}$$

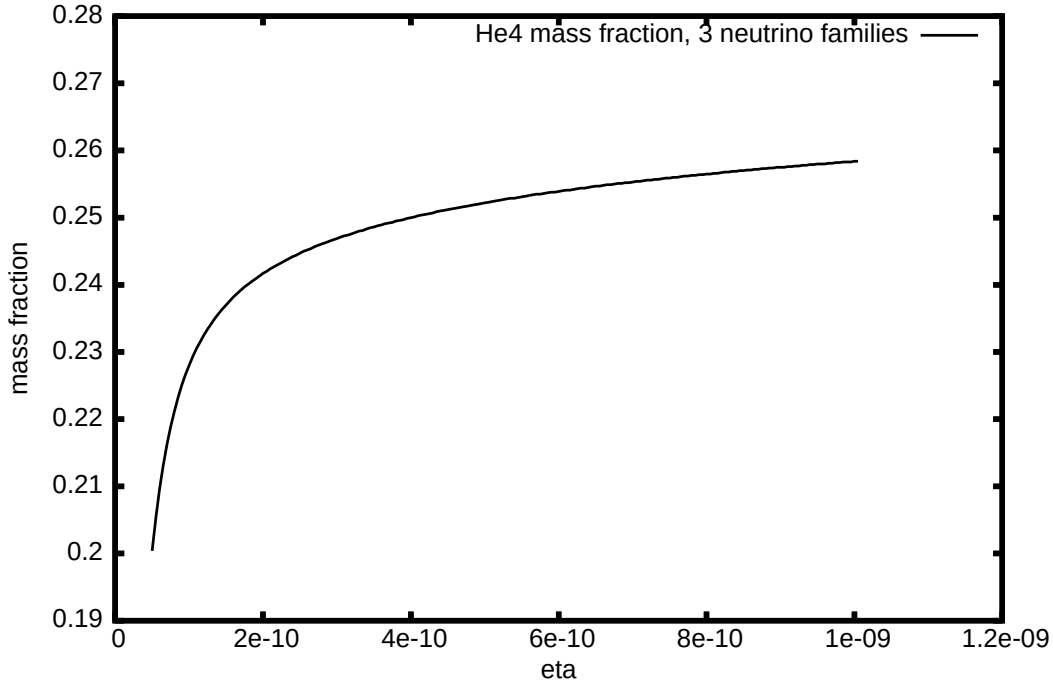


Figure 6: $^4$He production as a function of the baryon density

The recent all-sky, high precision measurement of the cosmic microwave background anisotropies by WMAP has opened the possibility for new precision analysis of BBN. Among other cosmological parameters, WMAP derived the baryon density with unprecedented precision [13] - [14]. The WMAP best fit assuming a varying spectral index is equivalent to $\eta_{10,\mathrm{WMAP}} = 6.14 \pm 0.25$. Using this value, my calculations predict a primordial $^4$He mass fraction (for standard Big Bang) of $X_\alpha = 0.2546^{+0.0003}_{-0.0004}$. But since we want to find a upper limit for $N_\nu$, observational data has to be considered, which is difficult. The principle is to observe emission lines of HII regions (and other astrophysical sites) with low metallicity, which means they should be as old (and therefore "primordial") as possible. One of the biggest problems is to extrapolate these values to zero metallicity using suitable models of chemical evolution in stars and galaxies.

The values quoted for the primordial $^4$He abundance varied considerably over the last 15 years. The work of Pagel et al. [12] established the analysis techniques that others were soon the follow. The published results in these years all lie around $0.228 < X_\alpha < 2.444$, strongly depending on the assumed value of the equivalent width of He absorption lines. But this was not a prob-

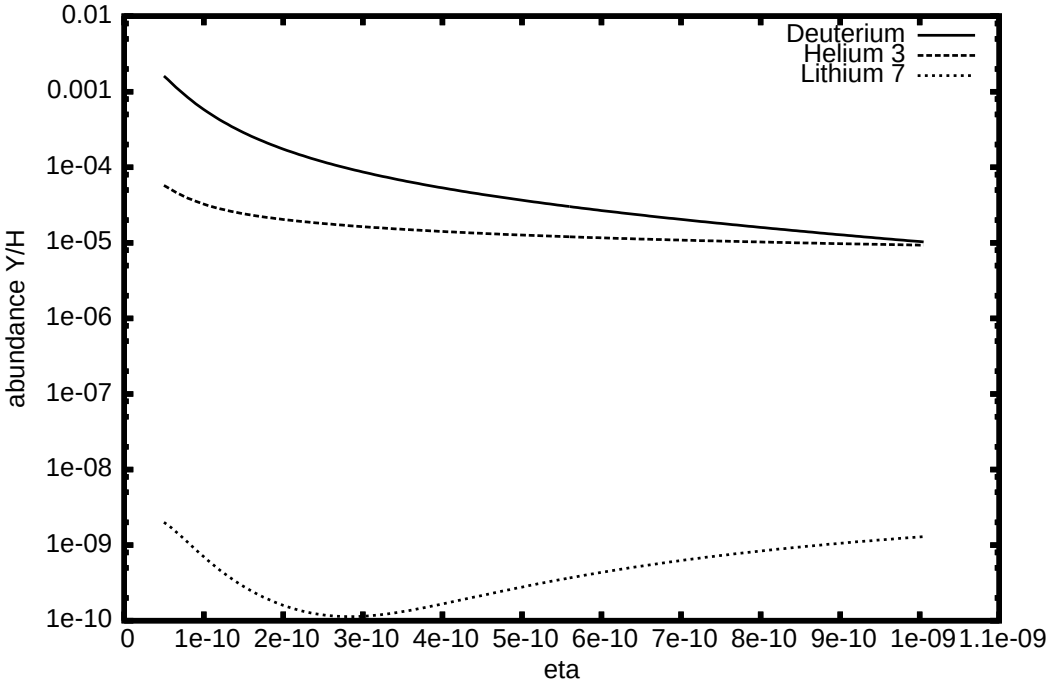


Figure 7: $^2$H, $^3$He and $^7$Li production as function of the baryon density

lem, since back then one believed $\eta_{10}$ to be in the narrow range between 2.8 and 4.0 (derived from observational D/H abundances). But since the analysis of the cosmic microwave background (CMB) became the most reliable source for baryon density determination, $\eta_{10}$ became significantly higher and therefore a reanalysis of the observed $^4$He became inevitable. Such a work from K.A. Olive et al. [11] led to an increased $X_\alpha$ value and also e bigger error range. A representative result of that analysis is

$$X_\alpha = 0.249 \pm 0.009 \tag{39}$$

Thus, conservatively, any value of $X_\alpha$ between 0.232-0.258 cannot be excluded. Consequently, using this constraint on $X_\alpha$ and the lower bound for $\eta_{10}$, the upper limit for $N_\nu$ becomes

$$N_\nu \lesssim 3.24 \quad , \tag{40}$$

based on our calculations. Here, uncertainties in the neutron mean life (small nowadays) are not considered. Nevertheless, this calculation clearly shows the unlikeliness of a $4^{th}$ neutrino family.

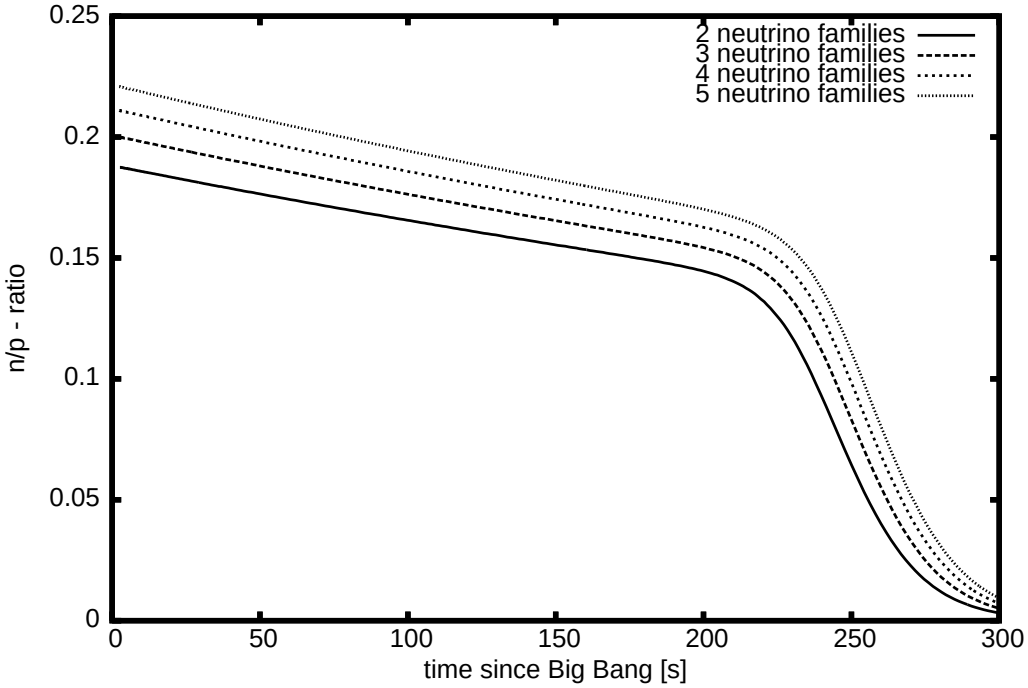


Figure 8: The evolution of the $n/p$ ratio: The more neutrino families we consider, the higher is this ratio at $T_{frz}$ and also at the time when BBN starts ($\sim 200s$)

# 5 Conclusion

Beginning with general cosmology, equations used for BBN have been modified in such a way that more than 3 neutrino families can be considered. Using these relations (depending on $\Delta N_\nu$) as input parameters for a full astrophysical network code, the impact of additional light neutrino families has been discussed (in addition to general BBN mechanisms). It has been found that additional light neutrino flavors increase the pressure of the plasma, resulting in a "speed-up" of cosmic expansion. It could be shown that this modification in spatial evolution has a significant influence on primordial abundances, especially on $^4$He.

Using observational data as a constraint for the primordial $^4$He mass fraction $X_\alpha$, an upper limit for $N_\nu$ could be determined: $N_\nu \lesssim 3.24$. As discussed in section 4, these results strongly depend on how observational data is interpreted, since with a different value of $X_\alpha$ the constraint on $N_\nu$ differs widely.

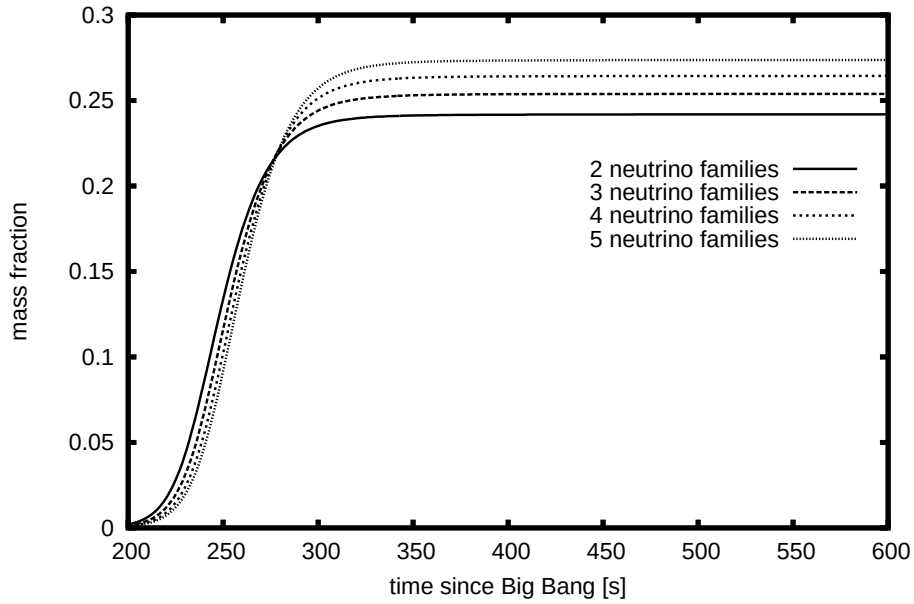


Figure 9: $^4$He production in detail

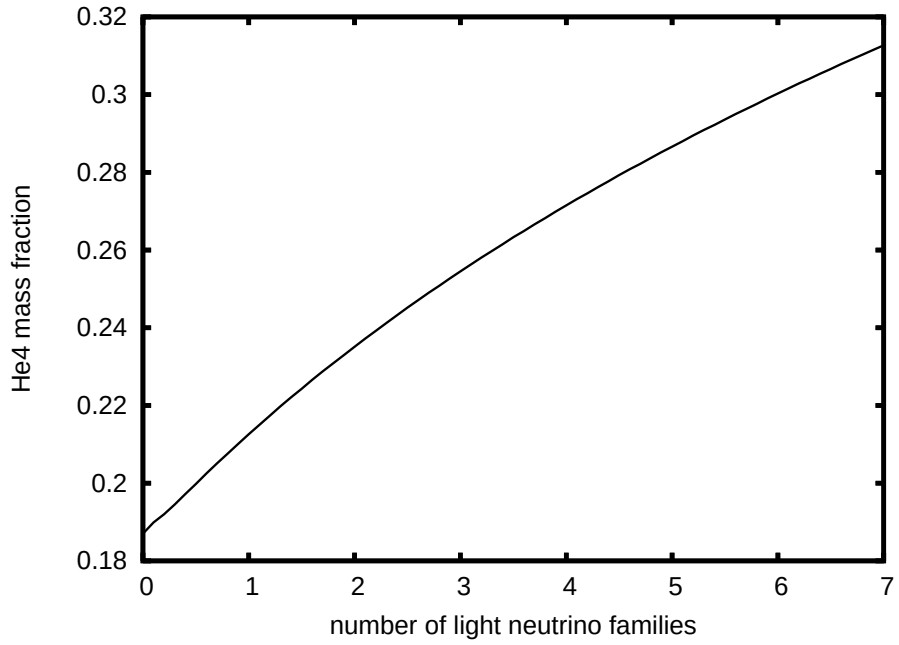


Figure 10: The predicted $^4$He mass fraction as a function of the number of neutrino families ($\eta_{10} = 6.14$)

# 6 Acknowledgments

At this place, I would like to thank especially Thomas Rauscher who assisted me with praiseworthy patience. I also appreciated the help of Carla Fröhlich, who supported me with the newest version of the network code and her know-how. Last but not least my thanks to F.-K. Thielemann for his ideas, talks and supervision.

# References

[1] "The Nuclear Evolution Of The Universe", Cowan, Thielemann, Truran, to be published

[2] "The Early Universe", E.W. Kolb, M.S. Turner, Perseus Publishing, Cambridge USA, 1990

[3] "Perspectives: Nucleosynthesis and Nuclear Reactions in Standard and Inhomogenous Big Bang Models and Beyon", F.K. Thielemann, M. Wiescher, in Proc. "Workshop On Primordial Nucleosynthesis", eds. W.J. Thompson, B.W. Carney, H.J. Karwowski, World Scientific, USA, 1989

[4] "Big Bang nucleosynthesis and physics beyond the standard model", Subir Sarkar, Rept. Prog. Phys. Vol. 59 (1996) p. 1493-1609

[5] "Model independent predictions of big bang nucleosynthesis from $^4$He and $^7$Li: consistency and implications". K. A. Olive, B. D. Fields, New Astronomy Vol. 1 (1996) p. 77-96

[6] "New BBN limits on physics beyond the standard model from $^4$He", R.H. Cyburt, B.D. Fields, K.A. Olive, Astroparticle Physics Vol. 23 (2005) p. 313-323

[7] "A new look at neutrino limits from big bang nucleosynthesis", K.A. Olive, G. Steigman, Physics Letters B Vol. 354 (1995) p. 357-362

[8] "Neutrinos and big bang nucleosynthesis", G. Steigman, Physica Scripta Vol. T121 (2005) p. 142-146

[9] "Precision neutrino counting", G. Steigman, eprint arXiv:astro/0108148v1 (2001)

[10] "Computational methods for nucleosynthesis and nuclear energy generation", W.R. Hix, F.-K. Thielemann, Journal of Computational and Applied Mathematics Vol. 109 (1999) p. 321-351

[11] "A Realistic Determination of the Error on the Primordial Helium Abundance: Steps Toward Non-Parametric Nebular Helium Abundances", K.A. Olive, E.D. Skillmann, Astrophys.J. Vol. 617 (2004) p. 29-49

[12] "Big Bang Nucleosynthesis - Observational Aspects", B.E.J. Pagel, Physica Scripta Vol. T36 (1991) p. 7-15

[13] "Cosmological Parameters from Cosmic Background Imager Observations and Comparisons with BOOMERANG, DASI, and MAXIMA", J.L. Sievers et al., Astrophys. J. Vol. 591 (2003) p. 599-622

[14] "Estimates of Cosmological Parameters Using the CMB Angular Power Spectrum of ACBAR", J.H. Goldstein, Astrophys. J. Vol. 599 (2003) p. 773-785